Domain Wall Dynamics under Nonlocal Spin-Transfer Torque

David Claudio-Gonzalez,* André Thiaville, and Jacques Miltat
Laboratoire de Physique des Solides, Université Paris-Sud, CNRS UMR 8502, 91405 Orsay, France
(Received 22 December 2011; published 1 June 2012)

We study spin-diffusion effects within a continuously variable magnetization distribution, integrating with micromagnetics the diffusive model of Zhang and Li [Phys. Rev. Lett. **93**, 127204 (2004)]. Current-driven wall motion is, in the steady velocity regime, shown to be adequately described by an effective nonlocal nonadiabatic parameter. This parameter is found to be 20% larger than its local counterpart for a vortex wall in a NiFe nanostrip and hardly modified for a transverse wall. This may account for the yet unexplained experimental evidence that vortex walls move more easily under current when compared with transverse walls. It is shown that this effective parameter can be derived from the domain wall structure at rest.

DOI: 10.1103/PhysRevLett.108.227208 PACS numbers: 75.78.Fg, 72.25.Ba, 75.76.+j, 75.78.Cd

Contrarily to charge, spin can accumulate in metals. The associated diffusion current flows in all directions, giving rise to nonlocal effects. Beyond transport properties [1,2], conduction electrons' spin resonance [3] and spin pumping [4] provide further testimonies for nonlocality in spin transport. These works all refer to samples consisting in piecewise uniform layers or blocks, magnetic or not. Of special significance to the present work is the noncollinear geometry where a spin current with polarization transverse to the magnetization exists, whose absorption in the vicinity of the surface of a magnetic layer creates a torque on the magnetization, known as spin-transfer torque (STT) [5]. Deciphering the behavior of samples exhibiting continuously variable properties, notably the magnetization orientation, is notoriously arduous since it requires a vector description of spin currents or of the transverse spin accumulation. Within a nanostrip, on the other hand, a moving domain wall (DW), because it concentrates all of the magnetization nonuniformity, acts as a built-in detector of spin torques [6]. The study of the STT-induced DW motion is further fueled by potential applications to data storage [7] and logic [8]. All in all, however, micromagnetics and spin-polarized transport need to be suitably admixed for a meaningful comparison between theoretical expectations and experiments.

The inclusion of STT into micromagnetics has up to now been performed with local terms that express the STT as a function of the local magnetization only. The magnetization dynamics is described by the classical Landau-Lifshitz-Gilbert (LLG) equation [9], augmented with a STT

$$\frac{\partial \vec{m}}{\partial t} = \gamma_0 \vec{H}_{\text{eff}} \times \vec{m} + \alpha \vec{m} \times \frac{\partial \vec{m}}{\partial t} - \vec{T}, \qquad (1)$$

with $\vec{m} = \vec{M}/M_s$ the unit vector along the local magnetization. The spin-transfer torque $\vec{T}$ in the local form is expressed as $\vec{T}_{\text{loc}} = u\partial_x \vec{m} - \beta u \vec{m} \times \partial_x \vec{m}$ $(\partial_x \equiv \partial/\partial x)$, where $u = JPg\mu_B/(2eM_s)$ is the velocity that represents the action of the spin-polarized current, with J the charge current density along the direction of the motion of electrons (x), P the spin polarization of the current, μ_B the Bohr magneton, and $e > 0$ the electronic charge. The second term of this torque, called nonadiabatic, is simply described by an additional factor without dimension called β. This term is necessary for obtaining steady-state DW motion under constant current, as the steady-state DW velocity v reads $v = (\beta/\alpha)u$ for any DW structure [10]. Whereas the adiabatic term determined by u is easily understood in the limit where the carriers' polarization exactly follows the local magnetization, the evaluation of β has stimulated many theoretical studies [11–16].

Some of the models have led to nonlocal STT forms. For the truly nonadiabatic term first, early ballistic transport calculations predicted a torque with an oscillatory spatial dependence [17]. This was confirmed by free electron models with exchange coupling to the local magnetization, owing to which a nonlocal torque was found [16,18,19] that corresponds to the so-called momentum transfer expected for atomically sharp DWs [11]. Because of the very small DW size necessary to observe such an effect, the influence of this torque term has not been studied in micromagnetics. When spin flip is taken into account, however, the presence of the diffusion term in the carriers' drift-diffusion equation implies that the spin density does not depend solely on the local magnetization. The relevant length scale (the spin-diffusion length) being closer to experimental DW sizes, measurable effects of a nonlocality of STT can be anticipated in this scheme. But this has not yet been tested, apart from two numerical solutions for the electrical current density and spin accumulation [20,21] with, in one case [20], coupling to the magnetization dynamics. However, these works pertain to nanopillars and as of yet have no experimental counterpart. Moreover, the quantitative differences with the case without carrier diffusion have not been singled out.

In this Letter, we quantitatively test the effects of spin diffusion, on real DW structures, by numerically

 © 2012 American Physical Society

implementing the Zhang-Li model into micromagnetics. As a first case, we investigate the steady-state velocity regime of DWs in NiFe soft nanostrips, applying current densities similar to those reported in experiments. In this regime, comparison to the analytical values obtained from the local model is indeed possible. Experimentally measured spin-diffusion parameters are used [22,23]. The nonequilibrium carriers spin density (hereafter spin density) $\delta\vec{m}$ is the solution of [12,24]

$$\frac{\partial \delta\vec{m}}{\partial t} = D\Delta\delta\vec{m} + \frac{1}{\tau_{sd}}\vec{m}\times\delta\vec{m} - \frac{1}{\tau_{sf}}\delta\vec{m} - u\partial_x\vec{m}. \quad (2)$$

Through the exchange interaction between carriers and local magnetization, the spin density exerts on the magnetization a spin-transfer torque $\vec{T} = (\vec{m}\times\delta\vec{m})/\tau_{sd}$. The local solution of Eq. (2), namely with $D = 0$ and no time derivative, yields the two local STT terms with $\beta = \tau_{sd}/\tau_{sf}$ [and a renormalized velocity $u_{ZL} = u/(1+\beta^2)$]. Two characteristic lengths are defined by this equation: the diffusion length during the spin-flip time τ_{sf}, $\lambda_{sf} = \sqrt{D\tau_{sf}}$, that is close to the spin-diffusion length of current perpendicular-to-plane giant magnetoresistance, and the diffusion length during the *s-d* exchange time $\tau_{sd} = h/J_{ex}$, usually denoted $\lambda_J = \sqrt{D\tau_{sd}}$ (see Ref. [24] for a discussion of the validity of this description of the effect of *s-d* exchange). One nice feature of Eq. (2) is its similarity to the LLG equation for magnetization dynamics, so that it can be solved with the same numerical methods (actually, this is not exactly so as $\delta\vec{m}$ is orthogonal to $\vec{m}$, is not normalized, and is assumed to create no demagnetizing field). We solve Eqs. (2) and (1) simultaneously, based on a homemade code developed for the LLG equation [25].

The sample considered is a 300 nm wide (y direction), 5 nm thick (z direction) NiFe soft nanostrip, a material and size much used in experiments [26,27]. At this size, the two main DW structures, the asymmetric transverse wall [ATW, Fig. 1(a)] and the vortex wall [VW, Fig. 2(a)] have nearly equal energies [28]. For the magnetization dynamics Eq. (1), a moving calculation box is used [29] in order to keep the DW always at its center. The numerical mesh size is $3\times3\times5$ nm^3, and the calculation box has a length (x direction) of 1200 or 3172 nm. Free boundary conditions apply for Eq. (2). The micromagnetic parameters correspond to the soft NiFe alloy: magnetization density $M_s = 8\times10^5$ A/m, anisotropy $K = 0$, exchange constant $A = 1\times10^{-11}$ J/m, gyromagnetic ratio $\gamma_0 = 2.21\times10^5$ m/C, and damping factor $\alpha = 0.02$ [29]. The nominal transport parameters derive from $\lambda_{sf} = 5$ nm [22], and $\lambda_J = 1$ nm [23] (hence $\beta = 0.04$), with $D = 0.25\times10^{-3}$ m^2/s [30]. The simulations methodology is as follows: we start at $t = 0$ with a micromagnetically converged DW under zero current and solve the LLG equation (1) together with the spin-density equation (2) simultaneously, under a constant u. The simulation times

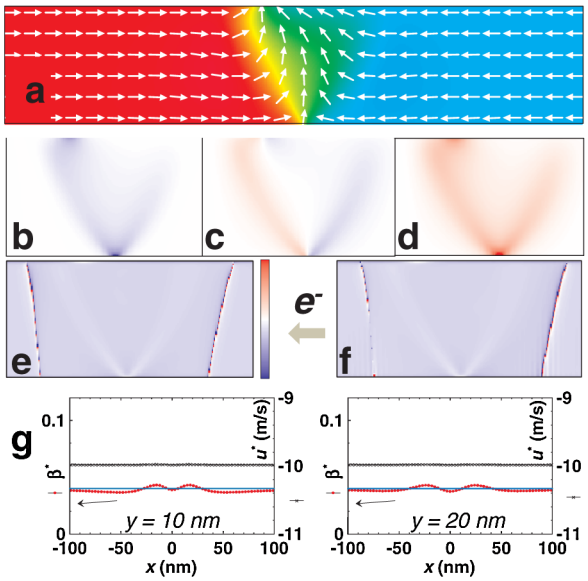

FIG. 1 (color online). Calculation results for an ATW in a NiFe nanostrip with 300×5 nm^2 cross section. (a) Magnetization structure of the ATW at rest, colored according to the inplane magnetization angle. (b)–(d) Nonequilibrium spin density for the DW at rest, obtained with $\tau_{sd}/\tau_{sf} = 0.04$ and $u = -10$ m/s, shown by its three components along x (b), y (c), and z (d). The color scale spans $\pm3\times10^{-5}$ for the inplane components and $\pm5\times10^{-4}$ for the z component. (e)–(f) Maps of β^* obtained for the DW at rest (e), and moving at steady velocity (f), the colors spanning the 0–0.1 interval. The color scale for images (b)–(f) is shown in the center, as well as the direction of motion of the carriers. All images have the same 300 nm height. (g) Plot of β^* and u^* along two horizontal lines, close to the tip of the ATW, for the DW structure at rest. The line shows the local value $\beta = 0.04$.

required to reach DW motion at a steady velocity are in the range of 5–100 ns, where the longest times correspond to the VW [32]. Equation (2), that contains time constants as small as 4 fs, requires a very small time step $\Delta t \approx 0.2$ fs, 10–100 times smaller than the typical value for micromagnetics [25]. We however describe in the Supplemental Material [33] how it is possible, in certain limits, to accelerate the calculations by keeping a typical micromagnetic time step.

The spin densities are shown in Figs. 1(b)–1(d) for the ATW and Figs. 2(b)–2(d) for the VW. They were calculated for the equilibrium DW structures. Using other values of the diffusion constant, e.g., 0 or 10 times higher, gives only slightly different maps, as the local solution dictates the overall shape of the spin density. In agreement with expectations derived from the local solution, the inplane densities are of order β for an inplane magnetization, whereas the out-of-plane (z) component is of order unity. In the vicinity of the vortex core with perpendicular magnetization, a contribution of order unity appears in the x component [Fig. 2(b)]. In order to better visualize the qualitative differences due to spin diffusion, we project

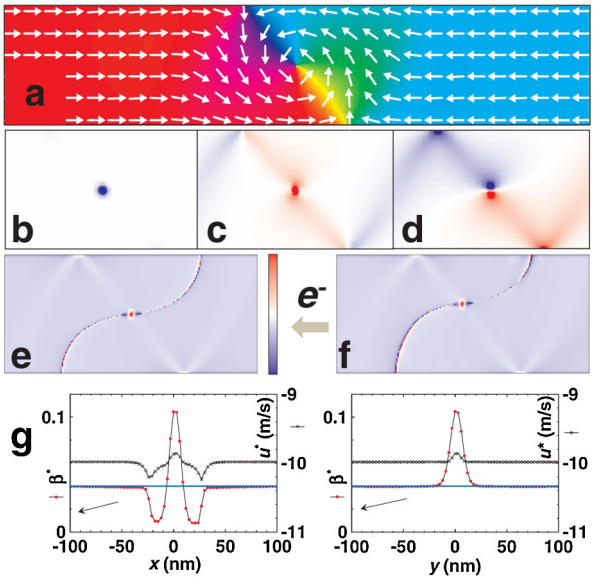

FIG. 2 (color online). Same results as in Fig. 1, for the case of a VW. The spin-density color range has become the large one for the x component (b). The plots (g) of β^* and u^* now correspond to horizontal and vertical lines across the vortex core. Note that the scales are identical to those of Fig. 1.

the nonequilibrium spin density $\delta\vec{m}$ onto the two components of the local solution, namely $\vec{m} \times \partial_x \vec{m}$ and $\partial_x \vec{m}$ (both orthogonal to $\vec{m}$ so that no information is lost). Thus we define

$$u^* = -\frac{\delta\vec{m} \cdot (\vec{m} \times \partial_x \vec{m})}{\tau_{\mathrm{sd}} |\partial_x \vec{m}|^2}, \qquad (\beta u)^* = -\frac{\delta\vec{m} \cdot \partial_x \vec{m}}{\tau_{\mathrm{sd}} |\partial_x \vec{m}|^2}. \quad (3)$$

The first projection represents a nonuniform spin-polarized current density u^*, and the second a nonuniform $(\beta u)^*$. Upon division we may evaluate a nonuniform nonadiabatic coefficient β^*. Maps of β^* for the ATW and VW are shown in Figs. 1 and 2, respectively, for the DW at rest (e) and under stationary motion (f). The curved lines segments where a divergence appears are inherent to the projection Eq. (3), but physically meaningless (see Supplemental Material [33]). For a more quantitative view, numerical values of u^* and β^* are provided in the plots (g) obtained along some characteristic lines. The data reveal an increase of β^* in the regions with large magnetization gradient. The increase is barely noticeable in the inclined 90° DW-like regions of the ATW and VW. But around the vortex core, that is, the smallest magnetic structure in this material, the increase is close to a factor of 3 [Fig. 2(g)]. This result may seem counterintuitive, as the spin-density equation (2) looks at first sight like a diffusion equation, known to smear out gradients. However, the physics of inhomogeneous precession and diffusion has already been shown to be more subtle [34]. In comparison, the u^* maps are extremely uniform [less than ±2% variation around the vortex core—see Fig. 2(g)—and much less for the ATW—see Fig. 1(g)].

By examining the velocities of the DWs moving in steady conditions we observe that one remarkable effect of spin diffusion is that the steady-state DW velocities (v_{diff}) are higher than those predicted by the local solution of the Zhang and Li model for general $\tau_{\mathrm{sd}}/\tau_{\mathrm{sf}}$ ratio [12],

$$v_{\mathrm{ZL}} = \frac{\beta}{\alpha} \frac{u}{1+\beta^2}. \quad (4)$$

A comparative panorama of DW velocities is presented in Table I. As the velocities can be small, and a high precision is required, local solution control calculations were performed for selected cases. These velocities (v_{loc}) are virtually identical to the analytical expectation given by Eq. (4), testifying to the accuracy of the calculations. We recall that in the case $D = 0$, the steady-state velocities predicted by the local STT form are independent of the DW configuration [10]. The numerical results show, however, that when taking into account spin diffusion, this is no longer the case. The velocities in the steady-state regime are replotted in Fig. 3 as a function of the applied current density (u), with the local value of β and the DW type as parameters. Note that the limited stability of the VW at this size (velocity bounded by $|v - u| < 61$ m/s [32]) prevents the use of large currents or large β values.

As seen from Table I and Fig. 3, the differences between the velocities predicted by the local solution of the Zhang and Li model and the full numerical solution for an ATW configuration are very small. However, for the VW configuration the differences are larger. This is illustrated in Fig. 3(a), where the velocities predicted by Eq. (4) are drawn for comparison by solid lines. We moreover observe that the computed velocities are consistent with an effective nonadiabatic parameter β_{diff} that depends only on the

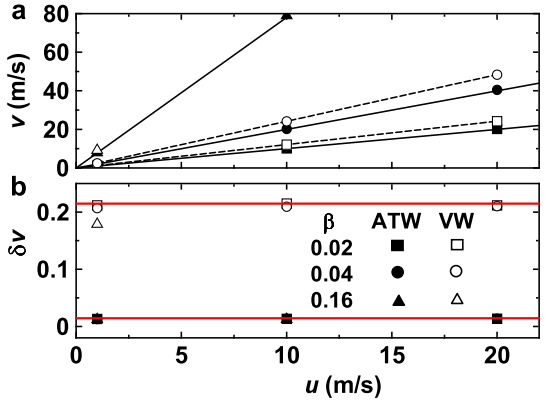

FIG. 3 (color online). Numerically computed steady-state DW velocities v as a function of u and for different values of τ_{sd} (hence β), for the ATW (filled symbols) and the VW (open symbols). (a) Comparison of the computed velocities with spin diffusion to the analytical results in the local approximation [Eq. (4), solid lines]. (b) Relative increase of velocity due to spin diffusion. The horizontal lines display the evaluation of β_{diff} from the weighted average of β^* computed for the DW structures at rest.

TABLE I. Steady-state DW velocities for different values of τ_{sd} ($\tau_{sf} = 100$ fs), spin-polarized current density u, DW type, and diffusion constant D (v_{loc}: $D = 0$ and v_{diff}: $D \neq 0$ [30], v_{ZL} being the analytic value for the local model). The damping constant is $\alpha = 0.02$. All velocities are in m/s [42], and the velocity increase due to electrons diffusion $\delta v = (v_{diff} - v_{ZL})/v_{ZL}$ is in percent.

τ_{sd}/τ_{sf}	u	DW	v_{ZL}	v_{loc}	v_{diff}	δv
0.02	1	ATW	1.00	1.00	1.01	1.3
0.04			2.00	2.00	2.02	1.3
0.16			7.80	7.80	7.90	1.2
0.02		VW	1.00	1.00	1.21	21.2
0.04			2.00		2.41	20.7
0.16			7.80	7.79	9.20	17.9
0.02	10	ATW	10.00	9.99	10.13	1.3
0.04			19.97	19.97	20.24	1.3
0.16			78.00	78.00	78.98	1.3
0.02		VW	10.00		12.14	21.5
0.04			19.97	19.96	24.15	21.0
0.02	20	ATW	19.99	19.99	20.26	1.4
0.04			39.94	39.93	40.48	1.4
0.02		VW	19.99		24.23	21.2
0.04			39.94	39.86	48.34	21.0

DW structure, being larger than the local value by $\approx 1\%$ for the ATW and by $\approx 20\%$ for the VW [Fig. 3(b)]. The parameter β_{diff} can be seen as a properly weighted average over the spatial distribution of the β^* parameter shown in Figs. 1 and 2. In fact, a rederivation of the Thiele equation proves that, in the case where $u^* \simeq u$, the weight function is simply $|\partial_x \vec{m}|^2$ (see Supplemental Material [33]). The β_{diff} values predicted by a calculation of the spin density for the DW at rest are indicated in Fig. 3(b), showing good agreement with the calculations even for non-zero DW velocities [35]. Thus, the effect of spin diffusion on STT-induced DW motion at low currents can be quantitatively evaluated *on the DW structure at rest*, similarly to the field-induced motion case owing to Thiele's approach [36]. The procedure is (i) compute the nonequilibrium spin density $\delta\vec{m}$ with the DW at rest, solving Eq. (2) to convergence or directly its time-independent version (see Supplemental Material [33]); (ii) compute the β^* distribution from Eq. (3); and (iii) compute β_{diff} by averaging with the $|\partial_x \vec{m}|^2$ weight function.

Therefore, a simultaneous solution of the diffusive Zhang and Li model together with the magnetization dynamics equation has uncovered a qualitatively new feature of the spin-transfer torque effect in the presence of spin diffusion, namely the dependence of the steady-state DW velocity on DW structure. We show that an effective nonadiabatic parameter β_{diff}, dependent on the DW structure, provides a good description of the phenomena, at least in the steady-state regime. The increase of DW velocity can be as high as 21% for NiFe nanostrips using realistic parameters. This increase is related to the presence in the DW structure of significant magnetization gradients over the characteristic length scales of the Zhang-Li equation, namely, the diffusion lengths related to spin flip and *s-d* exchange, as shown by an independent analytical work by A. Manchon and co-workers [37]. This may explain why VWs are more mobile than ATWs under STT, a feature observed experimentally but not predicted by the local STT in a perfect structure. Further studies are required to understand the modification of the nonsteady DW dynamics by spin diffusion, which is anticipated to be important as fine magnetic structures like antivortices are known to occur [29,38].

These results open another possibility to control STT by modifying the diffusion of the carriers. A related approach was experimentally tried by Lepadatu *et al.* [39]. where the β parameter was shown to be modified by changing the material's transport properties by doping. In addition, these results offer a starting point to study multilayer structures like spin-valve nanostrips [40,41], where the understanding of the observed increased efficiency of STT to drive DWs still remains elusive.

We acknowledge financial support and scientific discussions from the European network MRTN-CT-2006-035327 SPINSWITCH. D. C. G. acknowledges financial support from the Mexican Secretariat of Public Education SEP-PROMEP-NPTC-UGTO-PTC-180.

*Now at Department of Multidisciplinary Studies, University of Guanajuato, Mexico.

[1] T. Valet and A. Fert, Phys. Rev. B **48**, 7099 (1993).
[2] F. Jedema, A. Filip, and B. van Wees, Nature (London) **410**, 345 (2001).
[3] A. Janossy and P. Monod, Phys. Rev. Lett. **37**, 612 (1976).
[4] G. Woltersdorf, O. Mosendz, B. Heinrich, and C. H. Back, Phys. Rev. Lett. **99**, 246603 (2007).
[5] J. Slonczewski, J. Magn. Magn. Mater. **159**, L1 (1996).
[6] L. Berger, Phys. Rev. B **54**, 9353 (1996).
[7] S. Parkin, M. Hayashi, and L. Thomas, Science **320**, 190 (2008).
[8] D. Allwood, G. Xiong, C. Faulkner, D. Atkinson, D. Petit, and R. Cowburn, Science **309**, 1688 (2005).
[9] A. Hubert and R. Schäfer, *Magnetic Domains* (Springer Verlag, Berlin, 1998).
[10] A. Thiaville, Y. Nakatani, J. Miltat, and Y. Suzuki, Europhys. Lett. **69**, 990 (2005).
[11] G. Tatara and H. Kohno, Phys. Rev. Lett. **92**, 086601 (2004).
[12] S. Zhang and Z. Li, Phys. Rev. Lett. **93**, 127204 (2004).
[13] J. Xiao, A. Zangwill, and M. D. Stiles, Phys. Rev. B **73**, 054428 (2006).
[14] O. Wessely, D. M. Edwards, and J. Mathon, Phys. Rev. B **77**, 174425 (2008).
[15] I. Garate, K. Gilmore, M. D. Stiles, and A. H. MacDonald, Phys. Rev. B **79**, 104416 (2009).

[16] S. Bohlens and D. Pfannkuche, Phys. Rev. Lett. **105**, 177201 (2010).
[17] X. Waintal and M. Viret, Europhys. Lett. **65**, 427 (2004).
[18] G. Tatara, H. Kohno, J. Shibata, Y. Lemaho, and K.-J. Lee, J. Phys. Soc. Jpn. **76**, 054707 (2007).
[19] T. Taniguchi, J. Sato, and H. Imamura, Phys. Rev. B **79**, 212410 (2009).
[20] K. Matsushita, J. Sato, and H. Imamura, J. Appl. Phys. **105**, 07D525 (2009).
[21] N. Strelkov, A. Vedyayev, N. Ryzhanova, D. Gusakova, L. D. Buda-Prejbeanu, M. Chshiev, S. Amara, N. de Mestier, C. Baraduc, and B. Dieny, Phys. Rev. B **84**, 024416 (2011).
[22] J. Bass and W. Pratt, Jr., J. Phys. Condens. Matter **19**, 183201 (2007).
[23] T. Taniguchi, S. Yakata, H. Imamura, and Y. Ando, IEEE Trans. Magn. **44**, 2636 (2008).
[24] S. Zhang, P. M. Levy, and A. Fert, Phys. Rev. Lett. **88**, 236601 (2002).
[25] J. Miltat and M. Donahue, *Handbook of Magnetism and Advanced Magnetic Materials* (Wiley, New York, 2007), p. 742.
[26] M. Hayashi, L. Thomas, C. Rettner, R. Moriya, and S. Parkin, Nature Phys. **3**, 21 (2006).
[27] W. Uhlig, M. Donahue, D. Pierce, and J. Unguris, J. Appl. Phys. **105**, 103902 (2009).
[28] Y. Nakatani, A. Thiaville, and J. Miltat, J. Magn. Magn. Mater. **290–291**, 750 (2005).
[29] Y. Nakatani, A. Thiaville, and J. Miltat, Nature Mater. **2**, 521 (2003).
[30] There are no measurements of the diffusion constant of electrons in NiFe, but only estimates. The value $D = 10^{-3}$ m^2/s is quoted in Ref. [24] as typical. Einstein's relation $D = 1/[e^2\rho N(E_F)]$ may be used to estimate D, with the density of states obtained by the specific heat, but only at low temperature [31]. We started from $J_{ex} = 1$ eV and $\lambda_J = 1$ nm [23] to get $D = 2.5 \times 10^{-4}$ m^2/s.
[31] J. Lin and L. Kao, J. Phys. Condens. Matter **13**, L119 (2001).
[32] A. Thiaville, Y. Nakatani, F. Piéchon, J. Miltat, and T. Ono, Eur. Phys. J. B **60**, 15 (2007).
[33] See Supplemental Material at http://link.aps.org/supplemental/10.1103/PhysRevLett.108.227208 for numerical details and the derivation of the relation between the local β^* and the global β_{diff}.
[34] C. Deutsch, F. Ramirez-Martinez, C. Lacroûte, F. Reinhard, T. Schneider, J. N. Fuchs, F. Piéchon, F. Laloë, J. Reichel, and P. Rosenbusch, Phys. Rev. Lett. **105**, 020401 (2010).
[35] The deviations at very small u for the VW are attributed to mesh friction impeding the transverse motion of the vortex core.
[36] A. Thiele, Phys. Rev. Lett. **30**, 230 (1973).
[37] A. Manchon, W.-S. Kim, and K.-J. Lee, arXiv:1110.3487.
[38] J.-Y. Lee, K.-S. Lee, S. Choi, K. Y. Guslienko, and S.-K. Kim, Phys. Rev. B **76**, 184408 (2007).
[39] S. Lepadatu, J. S. Claydon, C. J. Kinane, T. R. Charlton, S. Langridge, A. Potenza, S. S. Dhesi, P. S. Keatley, R. J. Hicken, B. J. Hickey, and C. H. Marrows, Phys. Rev. B **81**, 020413(R) (2010).
[40] J. Grollier, P. Boulenc, V. Cros, A. Hamzić, A. Vaurès, and A. Fert, Appl. Phys. Lett. **83**, 509 (2003).
[41] S. Pizzini, V. Uhlíř, J. Vogel, N. Rougemaille, S. Laribi, V. Cros, E. Jiménez, C. Tieg, E. Bonet, M. Bonfim, R. Mattana, C. Deranlot, F. Petroff, C. Ulysse, and A. Fert, Appl. Phys. Express **2**, 023003 (2009).
[42] The raw velocity values were all corrected for an ''autodrift'' value that appears in the calculations, essentially for the ATW. This phenomenon is linked to an incomplete balance of the magnetostatic charges in asymmetric DW structures. The autodrift was removed by reversing DW asymmetry, current direction, or vortex core polarity, whichever applicable.